Electronic Supplementary Information (ESI) for

Precisely-controlled preparation of the advanced $Na_3V_2(PO_4)_2O_2F$ cathode material for sodium ion batteries: the optimization of electrochemical properties and electrode kinetics

Zhen-Yi Gu[ac], Jin-Zhi Guo[b], Yang Yang[b], Hai-Yue Yu[b], Xiao-Tong Xi[b], Xin-Xin Zhao[b], Hong-Yu Guan[d], Xiaoyan He*[c] and Xing-Long Wu*[ab]*

[a] *Key Laboratory for UV Light-Emitting Materials and Technology of Ministry of Education, Northeast Normal University, Changchun, Jilin 130024, P. R. China, E-mail: xinglong@nenu.edu.cn*

[b] *National & Local United Engineering Laboratory for Power Batteries, Department of Chemistry, Northeast Normal University, Changchun, Jilin 130024, P. R. China*

[c] *College of Chemistry and Environmental Science, Yili Normal University, Yining, Xinjiang 835000, P. R. China, E-mail: hexy856@sina.com*

[d] *School of Chemistry and Chemical Engineering, Guangzhou University, Guangzhou 510006, China, E-mail: guanhy@nenu.edu.cn*

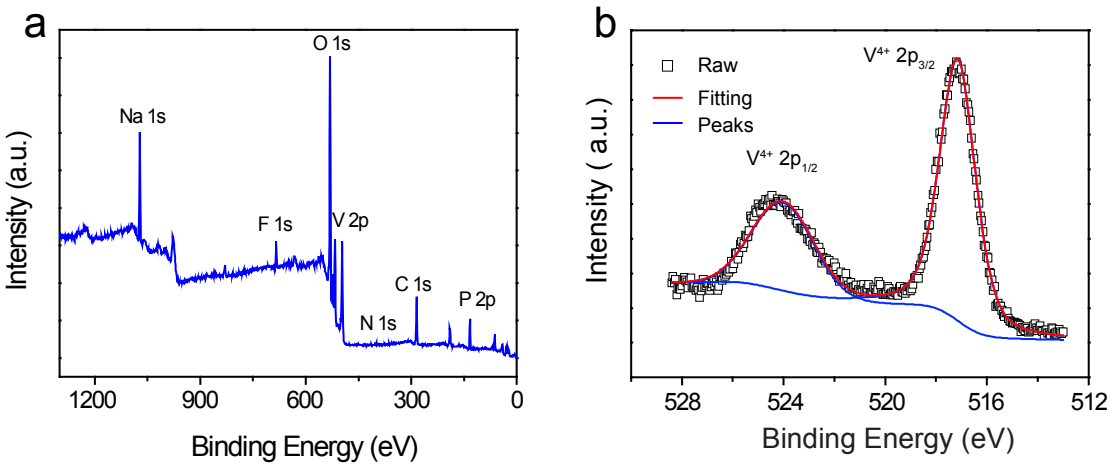

Figure S1. XPS spectrum of the optimally prepared NVPOF under 170 °C at pH = 7: (a) the overall and (b) high-resolution V2p spectra.

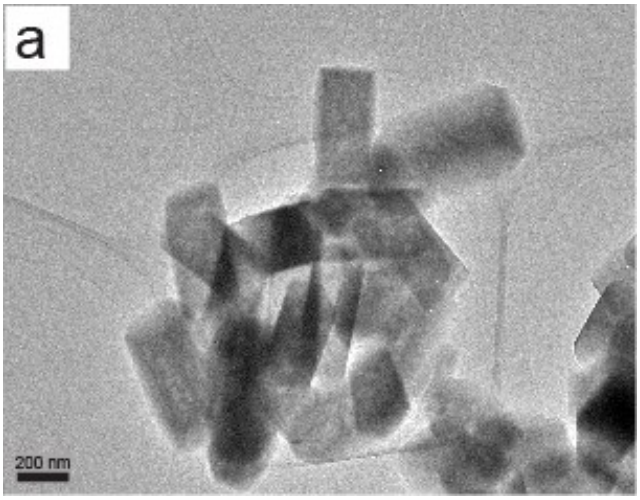

Figure S2.TEM images of the NVPOF materials prepared at 170 °C under pH=7.

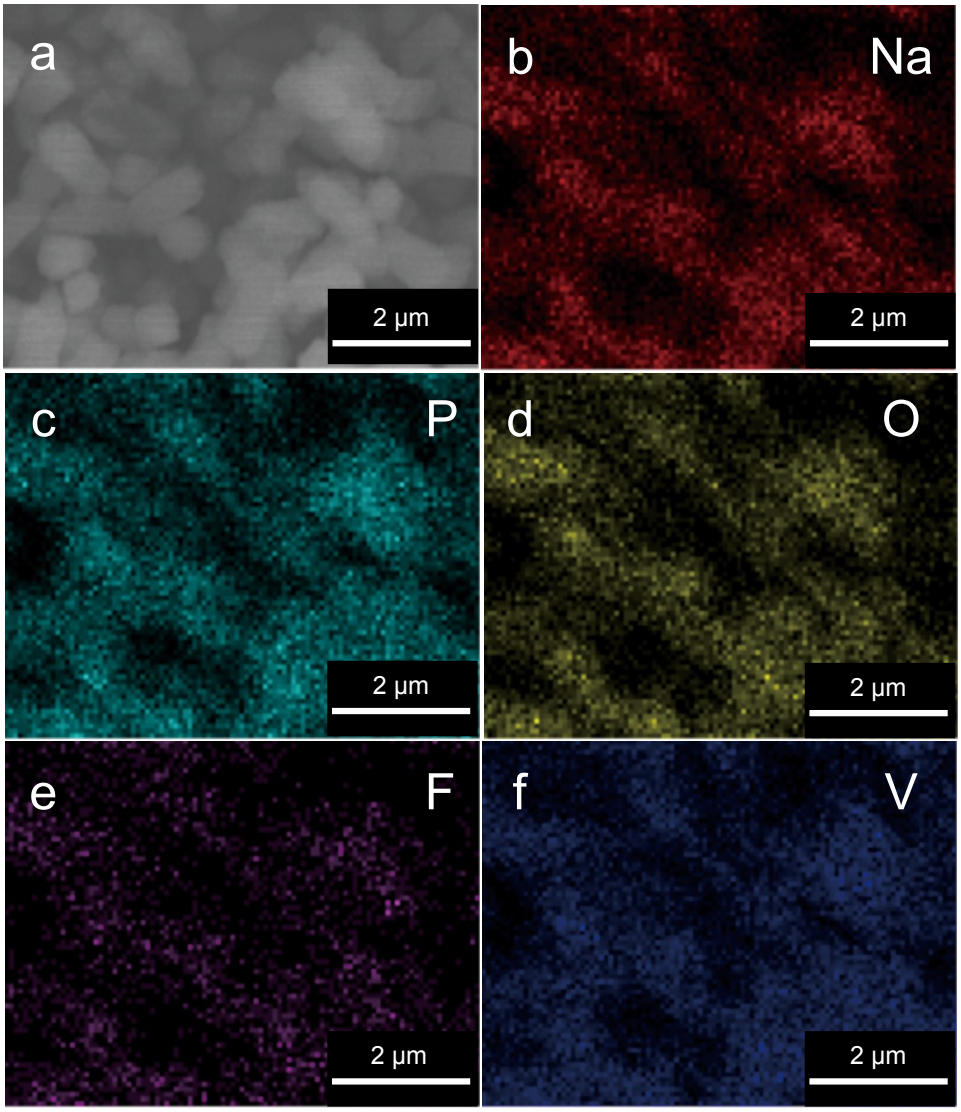

Figure S3. SEM image and the corresponding elemental mappings of the NVPOF material prepared at pH = 7 under 170 ^{o}C.

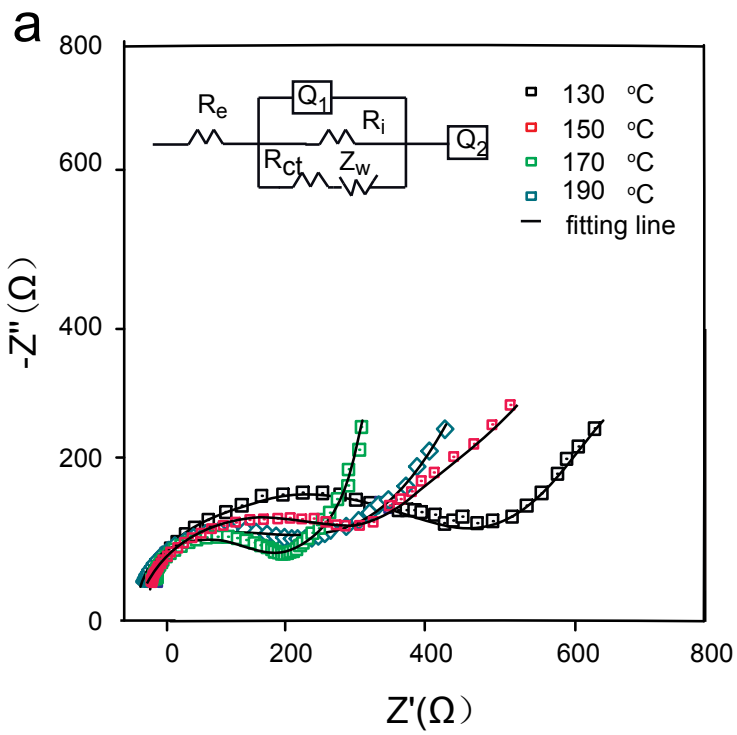

Figure S4. The impedance spectra (1 MHz ~ 10 mHz) of NVPOF at different temperatures and quivalent circuit used for curve fitting.

Table S1 Impedance parameters derived by using equivalent circuit model of the NVPOF materials prepared under different temperature

T/°C	R_s/Ω	R_{ct}/Ω
130	7.48	565
150	6.81	383
170	3.56	205
190	4.36	232

Table S2 Comparison of NVPOF materials from our work with previously reported ones of phosphate-based cathode materials for Na-ion batteries.

Materials	Synthesis methods	Elctrochemical activity	Ref
$Na_3V_2(PO_4)_3$	Solid-state reaction	116.5 mA h g^{-1} 3.4 V (Q_{Th} = 117 mA h g^{-1})	[1]
$NaVPO_4F$	Solid-state reaction	82 mA h g^{-1}, 3.7 V (Q_{Th} = 142.6 mA h g^{-1})	[2]
$NaV_{1-X}Cr_XPO_4F$	Solid-state reaction	83.3 mA h g^{-1}, 3–4.5 V (Q_{Th} = 142.6 mA h g^{-1})	[3]
$Na_3V_2(PO_4)_2F_3$	Carbothermal reduction	111.6 mAh g-1, 2.5–4.6 V (Q_{Th} = 128.2 mA h g^{-1})	[4]
$Na_3Ti_2(PO_4)F_3$	Solid-state reaction	57.7 mA h g^{-1}, 1.5–3.5 V (Q_{Th} = 132.8 mA h g^{-1})	[4]
$Na_{1.5}VO(PO_4)_2F$	Hydrothermal	100 mA h g^{-1}, 3.6–4 V (Q_{Th} = 156 mA h g^{-1})	[5]
$Na_3V_2O_2(PO_4)_2F$-G	Solvothermal	120 mA h g^{-1}, 2.5–4.5 V (Q_{Th} = 122.4 mA h g^{-1})	[6]
Na_2FePO_4F	Solid-state reaction	110 mA h g^{-1}, 2–3.8 V (Q_{Th} = 124.2 mA h g^{-1})	[7]
Na_2MnPO_4F	Solid-state reaction	100 mA h g^{-1}, 3.4 V (Q_{Th} = 124.7 mA h g^{-1})	[8]
Na_2CoPO_4F	Solid-state reaction	100 mA h g^{-1}, 4.3 V (Q_{Th} = 122.4 mA h g^{-1})	[9]
$NaFeSO_4F$	Solid-state synthesis	6 mA h g^{-1}, 3.5 V (Q_{Th} = 138 mA h g^{-1})	[10]
$Na_3V_2O_2(PO_4)_2F$	Hydrothermal	123 mA h g^{-1}，2-4.3V (Q_{Th} = 130 mA h g^{-1})	This work

Table S3 CV at various scan rates tests were employed to analyze the Na-migration kinetics of the NVPOF electrode to the Randles–Sevcik equation, and the $D_{app,Na}$ values.

	pH=5	pH=6	pH=7	pH=8
A1	3.71 E-11	1.18 E-10	2.56 E-10	1.64 E-10
A2	1.94 E-11	4.65 E-11	1.48E-10	7.27 E-11
C1	2.21 E-11	6.88 E-11	1.75 E-10	1.07 E-10
C2	7.87 E-12	1.51E-11	2.98 E-11	2.75 E-11

Calculation process for the apparent Na chemical diffusion coefficients through CV tests

The apparent Na diffusion coefficient ($D_{app,Na}$) was calculated from the following Randles-Sevcikequation S1:[11]

$$ip = 2.69 \times 10^5 n^{3/2} A D_{app,Na}^{1/2} C_0 v^{1/2} \quad \text{(S1)}$$

where *ip* is the peak current density, n is the electron-transfer number per molecule formula during the redox reaction (*n*= 2 for the present NVPOF),[12] *A* is the surface area of the electrode, C_0 is the concentration of Na ions in the electrode (7.7 mmol cm^{-3}),[13]and *v* is the scan rate.

Calculation process for the apparent Na chemical diffusion coefficients through GITT tests.

The $D_{app,Na}$ values can be calculated according to the following equation S2:[14]

$$D_{app,Na} = \frac{4}{\pi\tau}\left(\frac{m_B V_M}{M_B S}\right)^2\left(\frac{\Delta E_s}{\Delta E_\tau}\right)^2 \quad \text{(S2)}$$

where m_B, M_B,and V_M are the mass, molecular weight, and molar volume of the NVPOF material, respectively; τ is the time for an applied galvanostatic current; *S* is the active surface of the electrode; *L* is the average radius of the material particles; and ΔEs and $\Delta E\tau$ are the quasi-equilibrium potential and the change of cell voltage *E* during the current pulse, respectively.

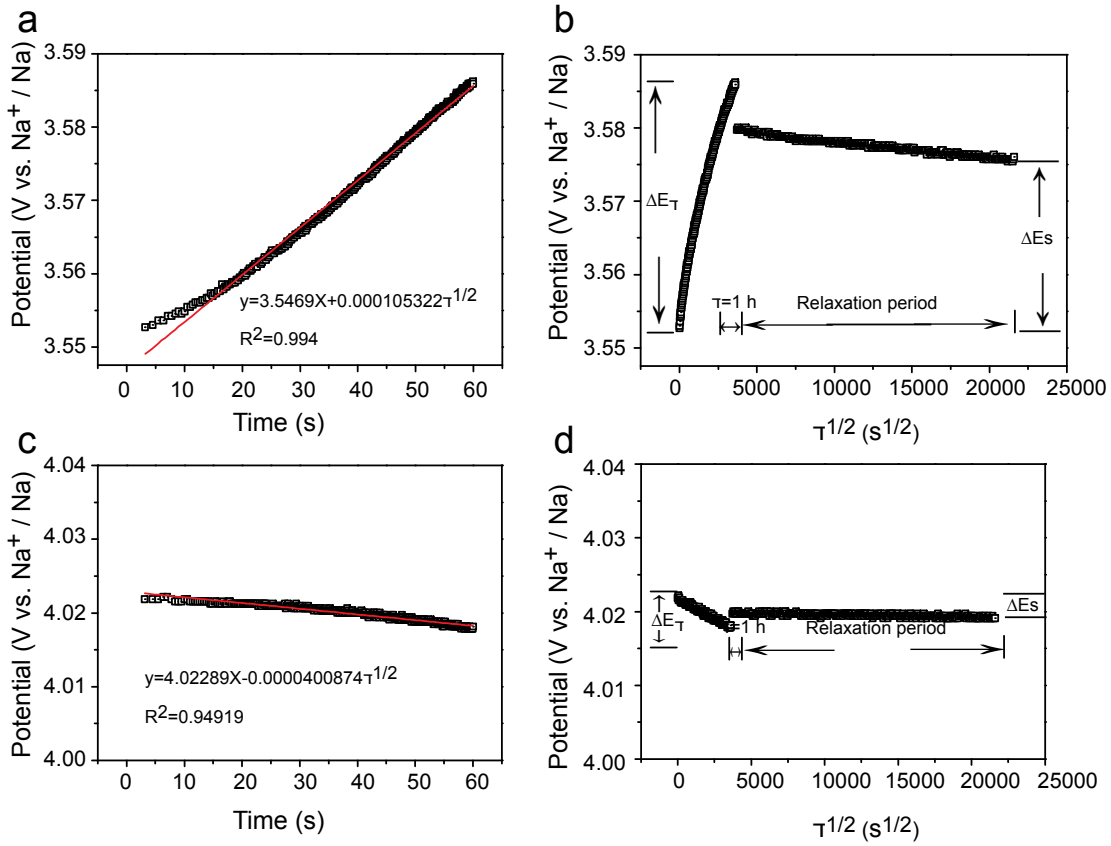

Figure S5. A sigle GITT profile for charge and discharge process.τ vs *E* profile for a single GITT titration during (b) charge and (d) discharge processes. The corresponding linearly fitting behavior of *E* vs $\tau^{1/2}$ for the (a) charge and (c) discharge GITT titration.

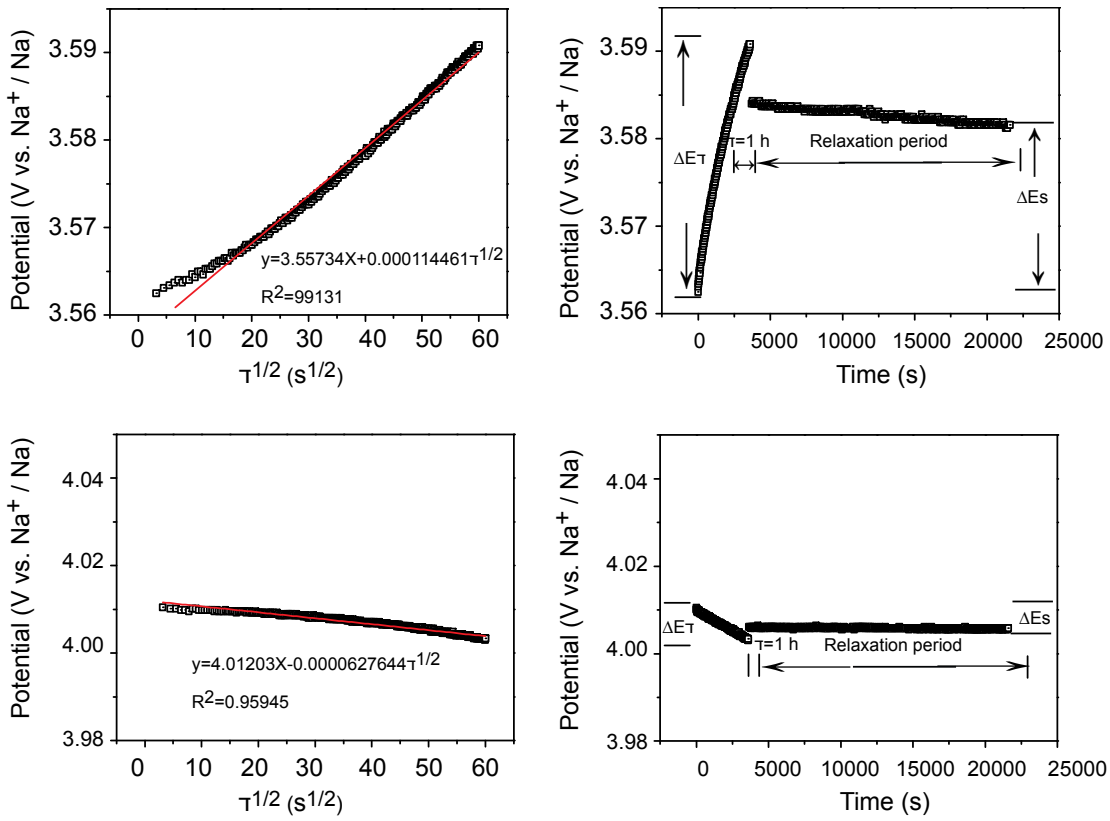

Figure S6. A sigle GITT profile for charge and discharge process.τ vs *E* profile for a single GITT titration during (b) charge and (d) discharge processes. The corresponding linearly fitting behavior of *E* vs $\tau^{1/2}$ for the (a) charge and (c) discharge GITT titration.

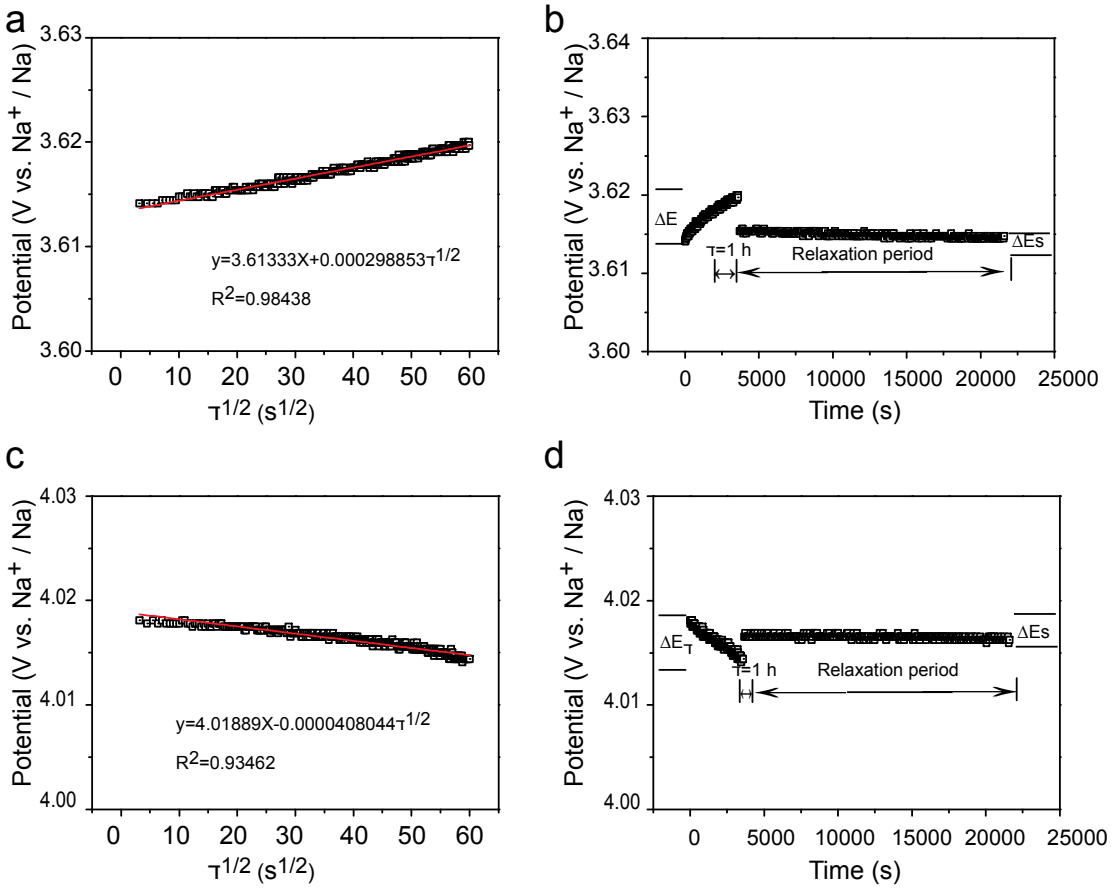

Figure S7. A sigle GITT profile for charge and discharge process.τ vs *E* profile for a single GITT titration during (b) charge and (d) discharge processes. The corresponding linearly fitting behavior of *E* vs $\tau^{1/2}$ for the (a) charge and (c) discharge GITT titration.

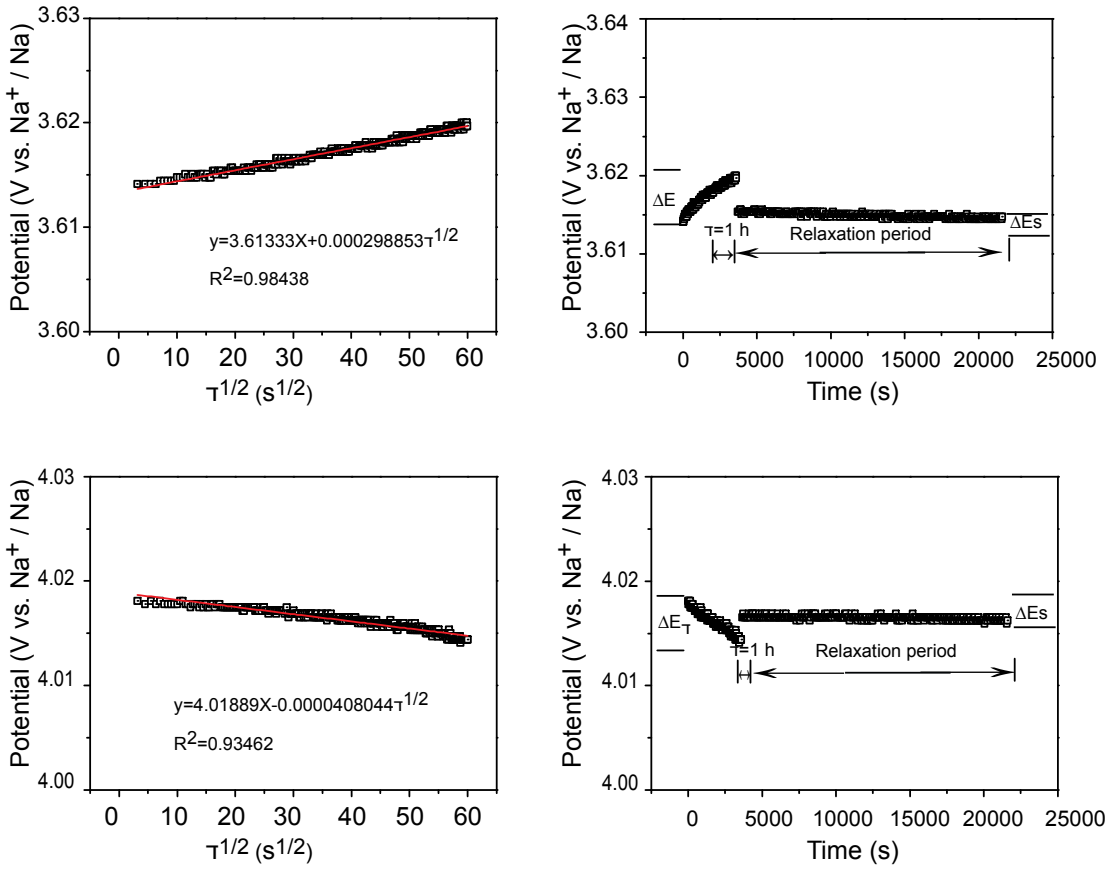

Figure S8. A sigle GITT profile for charge and discharge process.τ vs *E* profile for a single GITT titration during (b) charge and (d) discharge processes. The corresponding linearly fitting behavior of *E* vs $\tau^{1/2}$ for the (a) charge and (c) discharge GITT titration.

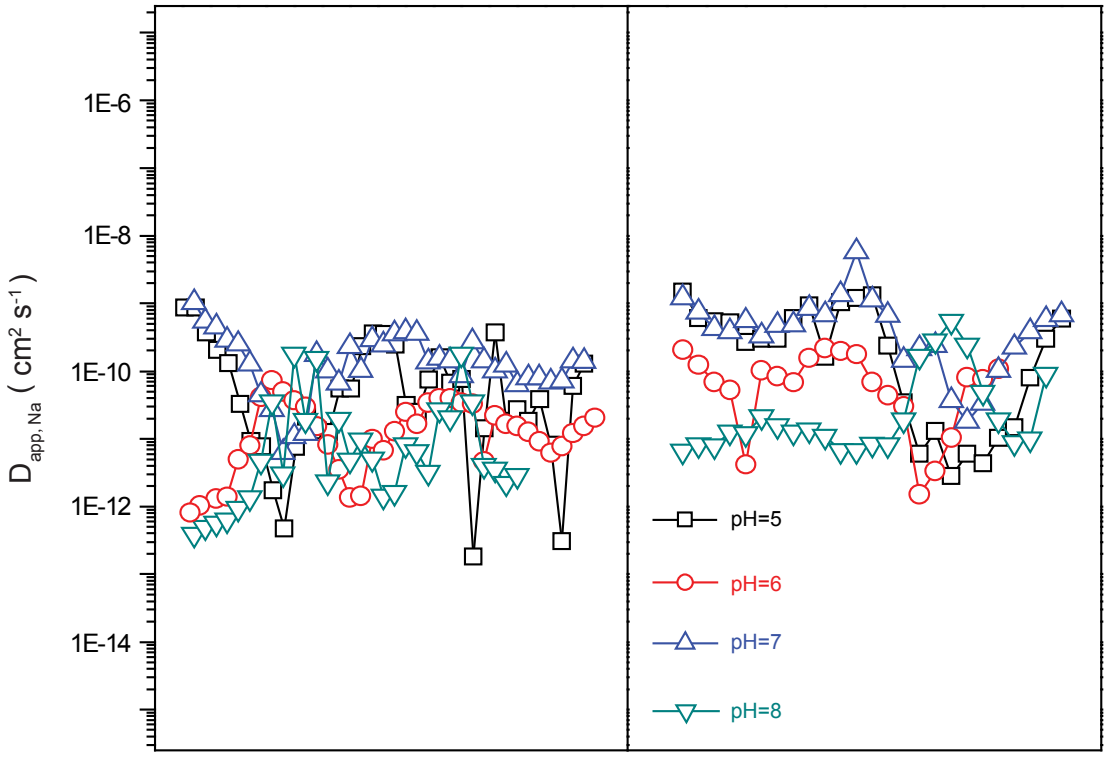

Figure S9. The comparison of $D_{app,Na}$ values obtained from GITT tests for the NVPOF materials prepared under different pH (5, 6, 7 and 8) at 170 °C.

ESI References

1 . Q. Hu, T. Y. Liao, and C. H. Chen, *J. Mater. Chem. A*., 2016, **4,** 16801-16804.

2 . J. Barker, M. Y. Saidi, J. L. Swoyer, *Electrochem. Solid-State Lett.*, 2003, **6**, A1.

3 . H. Zhou, X. Wang, A. Tang, Z. Liu, S. Gamboa, P. J. Sebastian, *J. Power Sources*, 2006, **160**, 698.

4 . W. Song, X. Cao, Z. Wu, J. Chen, Y. Zhu, H. Hou, Q. Lan, X. Ji, *Langmuir*, 2014, **30**, 12438.

5 . P. Serras, V. Palomares, A. Goni, I. Gil de Muro, P. Kubiak, L. Lezama, T. Rojo, *J. Mater. Chem.*, 2012, **22**, 22301.

6 . M. Xu, L. Wang, X. Zhao, J. Song, H. Xie, Y. Lu, JB. Goodenough, *Phys. Chem. Chem. Phys.*, 2013, **15**, 13032.

7 . Y. Kawabe, N. Yabuuchi, M. Kajiyama, N. Fukuhara, T. Inamasu, R. Okuyama, I. Nakai, S. Komaba, *Electrochem. Commun.*, 2011, **13**, 1225.

8 . S.-W. Kim, D.-H. Seo, H. Kim, K.-Y. Park, K. Kang, *Phys. Chem. Chem. Phys.*,

2012, **14**, 3299.

9 . K. Kubota, K. Yokoh, N. Yabuuchi, S. Komaba, *Electrochem.*, 2014, **82**, 909.

10 . P. Barpanda, J.-N. Chotard, N. Recham, C. Delacourt, M. Ati, L. Dupont, M. Armand, J.-M. Tarascon, *Inorg. Chem.*, 2010, **49**, 7401.

11 . K. Tang, X. Yu, J. Sun, H. Li, X. Huang, *Electrochim. Acta*, 2011, **56**, 4869.

12 . P. R. Kumar, Y. H. Jung, J. E. Wang, D. K. Kim, *J. Power Sources*, 2016, **324**, 421.

13 . W. Massa, O. V. Yakubovich, O. V. Dimitrova, *Solid State Sci.*, 2002, **4**, 495.

14 . S. Guo, H. Yu, Z. Jian, P. Liu, Y. Zhu, X. Guo, M. Chen, M. Ishida, H. Zhou, *ChemSusChem*, 2014, **7**, 2115.